Unexpected z-Direction Ising Antiferromagnetic Order in a Frustrated Spin-1/2 $J_1 - J_2$ XY Model on the Honeycomb Lattice

Zhenyue Zhu,[1] David A. Huse,[2] and Steven R. White[1]

[1]*Department of Physics and Astronomy, University of California, Irvine, California 92697, USA*

[2]*Physics Department, Princeton University, Princeton, New Jersey 08544, USA*

(Received 10 October 2013; revised manuscript received 24 November 2013; published 16 December 2013)

Using the density matrix renormalization group on wide cylinders, we study the phase diagram of the spin-1/2 XY model on the honeycomb lattice, with first-neighbor ($J_1 = 1$) and frustrating second-neighbor ($J_2 > 0$) interactions. For the intermediate frustration regime $0.22 \lesssim J_2 \lesssim 0.36$, we find a surprising antiferromagnetic Ising phase, with ordered moments pointing along the z axis, despite the absence of any $S_z S_z$ interactions in the Hamiltonian. Surrounding this phase as a function of J_2 are antiferromagnetic phases with the moments pointing in the $x - y$ plane for small J_2 and a close competition between an $x - y$ plane magnetic collinear phase and a dimer phase for large values of J_2. We do not find any spin-liquid phases in this model.

DOI: 10.1103/PhysRevLett.111.257201 PACS numbers: 75.10.Jm, 73.43.Nq, 75.10.Kt

The past few years have seen a major resurgence in both experimental and theoretical interest in quantum spin-liquid ground states [1]. Much of the interest stems from strong evidence that quantum spin liquids exist experimentally in several different materials [1]. In the case of the kagome lattice material herbertsmithite, $ZnCu_3(OH)_6Cl_2$, for example, mounting experimental evidence for a spin-liquid low temperature phase [2–6] has coincided with recent strong numerical evidence that the spin-1/2 Heisenberg kagome antiferromagnet has a spin-liquid ground state [7], and that this state has Z_2 topological order [8,9]. The numerical work has become possible through continued advances in density matrix renormalization group (DMRG) techniques; these methods can now be used to study frustrated spin Hamiltonians on cylinders with widths up to 12 or 14 lattice spacings, which, when combined with careful finite size analysis, can determine phases and properties in the two-dimensional thermodynamic limit with good confidence in many cases. There is great interest in understanding the kagome spin liquid in more detail, and in finding other spin liquids in simple realistic models.

Recently, Varney *et al.* [10] studied the spin-1/2 XY model on the honeycomb lattice, with first-neighbor ($J_1 = 1$, $\langle i, j\rangle$) and frustrating second-neighbor ($J_2 > 0$, $\langle\langle i, j\rangle\rangle$) XY interactions, with Hamiltonian

$$H = J_1 \sum_{\langle i,j\rangle} (S_i^+ S_j^- + \text{H.c.}) + J_2 \sum_{\langle\langle i,j\rangle\rangle} (S_i^+ S_j^- + \text{H.c.}). \quad (1)$$

Based on exact diagonalization (ED) of various small clusters, they suggested that a particular spin-liquid ground state, a "Bose liquid," appears for $0.21 \lesssim J_2 \lesssim 0.36$. Bose liquids may have a singular surface in momentum space, similar to a Fermi surface for a Fermi system, with gapless excitations and power-law correlations [11,12], or they may be gapped and incompressible [13,14]. This spin model is equivalent to spinless hard-core bosons with first- and second-neighbor hopping and zero off-site interactions. Our motivation for the present study was to examine much larger lattices to see whether we could determine if this system really has a spin-liquid ground state in some region of the phase diagram in the thermodynamic limit.

We have performed numerous DMRG [15–17] calculations on this model on long cylinders with circumferences up to 12 lattice spacings. The properties of the ground state are governed by the ratio J_2/J_1. In all of our calculations, we take $J_1 = 1$ and $0 \le J_2 \le 1$, thus antiferromagnetic interactions. The cylinder geometries we used in our DMRG calculations are adopted from Ref. [18]. For example, XC8 represents a cylinder where one set of edges of each hexagon lie along the x direction (which always coincides with the cylinder axis), and there are 8 spins along the circumferential zigzag columns, connected periodically (Fig. 1). The actual circumference (Euclidean distance) of XC8 is $C = 4\sqrt{3}$ lattice spacings. For the YC6 cylinder, one set of edges of each hexagon lies along the y (circumferential) direction and there are 6 spins (in 3 pairs) along a straight circumference of $C = 9$ lattice spacings [Fig. 2(b)]. For narrow cylinders like XC8, we are easily able to achieve a truncation error of about 10^{-8} with $M = 2400$ states, which determines the ground state essentially exactly. For YC8, our widest cylinder with $C = 12$, we need to keep $M = 5800$ to achieve a truncation error of 10^{-6}—still excellent accuracy. In all our DMRG calculations, we keep enough states to make sure that the truncation error is smaller than 10^{-6}.

In the unfrustrated limit of $J_2 = 0$, the ground state has the expected Néel order in the xy plane. We find that this phase extends to $J_2 \sim 0.22$. In the interval $0.22 \lesssim J_2 \lesssim 0.36$, we find an antiferromagnetic phase that surprisingly has staggered magnetization polarized along the z direction in spin space; we call this Ising antiferromagnetic order, to

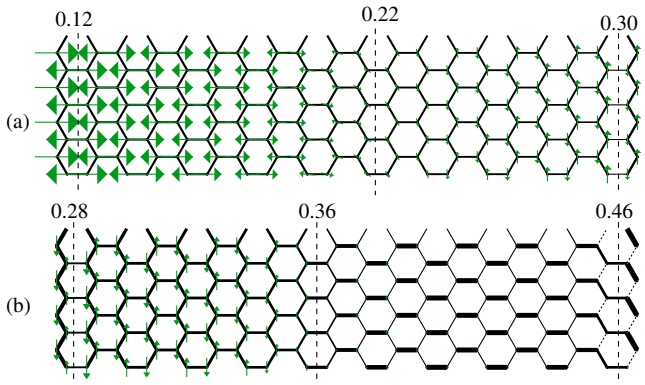

FIG. 1 (color online). (a) Local magnetic moments for an XC8 cylinder with J_2 varying along the length of the cylinder. The dashed lines show the locations of particular J_2 values. In (a), we show a cylinder with J_2 varying from 0.12 to 0.30. For $J_2 \sim 0.22$, the xy-plane Néel order rotates to z-direction Ising order. In (b), J_2 is varied from 0.28 to 0.46. The second phase transition point is located at $J_2 \sim 0.36$.

distinguish it from Néel order in the xy plane. Finally, for $J_2 \gtrsim 0.36$, we find that there is a close competition between a magnetically ordered xy-plane collinear phase and a magnetically disordered dimer phase. For example, on XC8 cylinders at $J_2 = 0.5$, the ground state is a dimer state, with energy $E = -0.3227$; see Fig. 2(a). A collinear state with an energy 1.2% higher on XC8 is metastable within DMRG. Similarly, on XC12 cylinders the ground state is also a dimer state with energy only 0.25% lower than the collinear state. However, on XC10, YC4, and YC6 cylinders, the ground state at $J_2 = 0.5$ is the collinear state, and the dimer state is not even metastable; see Fig. 2(b) for an illustration of the collinear ground state on the YC6 cylinder. The collinear states on different cylinders have relatively small finite size effects, with energy $E \cong -0.3189$. In this Letter, we will not try to resolve this close competition between these two states for $J_2 > 0.36$ in the 2D limit; instead, we will focus on the intermediate Ising phase regime.

From our DMRG calculations on large cylinders, we agree with Ref. [10] about the rough locations of the two phase boundaries and the properties of the phase for small J_2. However, in the intermediate phase we find long-range Ising antiferromagnetic order, which was not noticed in previous work on smaller systems. Thus we conclude that this system does not have a spin-liquid phase. In terms of bosons, this intermediate Ising phase has "charge-density" order of the bosons, with higher density on one sublattice than the other.

In Fig. 1, we present two cylinders to first give a quick summary of the whole phase diagram. These are XC8 cylinders in which J_2 is varied along the length of the cylinder, showing locally the various phases. In Fig. 1(a), J_2 varies from 0.12 to 0.30. At the $J_2 = 0.12$ left edge, a staggered field in the xy plane was applied to "pin" the Néel order. The ordered moments rotate from the x to the z direction, indicating that there is a phase transition between Néel and Ising order, at $J_2 \sim 0.22$. In Fig. 1(b), J_2 is varied from 0.28 to 0.46, with pinning bonds at the $J_2 = 0.46$ right end to pin dimer order. The phase transition from Ising to dimer order is visible at $J_2 \sim 0.36$. We also applied these methods to other cylinders and find that the values of J_2 at the estimated phase transitions change only slightly between different width and orientation cylinders. Thus, the locations of these phase transitions show only small finite size effects, which is consistent with our agreement with the small-size ED results from Ref. [10].

We have tested the stability of the Ising phase in several ways. For example, one can measure the decay of the local staggered magnetization away from an applied staggered field on an end of the cylinder. For the Néel ordered phase (small J_2), when we apply the pinning magnetic field along the z direction, $|\langle S_z \rangle|$ decays exponentially from the cylinder end [Fig. 3(a)]. To similarly test the Ising phase, we apply the pinning field along the x direction at the ends of

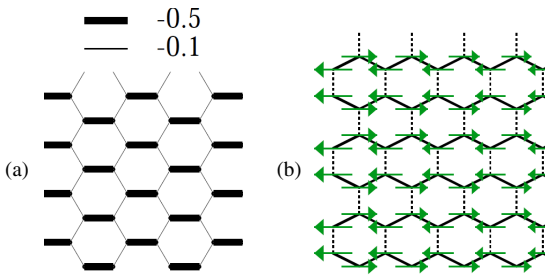

FIG. 2 (color online). (a) The ground state on the XC8 cylinder at $J_2 = 0.5$, showing strong dimer correlations aligned horizontally. We call this state a dimer state. (b) The ground state on YC6 cylinder at $J_2 = 0.5$. It has xy-plane collinear magnetic order, with antiferromagnetic chains along the horizontal zigzag direction together with ferromagnetic first-neighbor correlations between these zigzag chains.

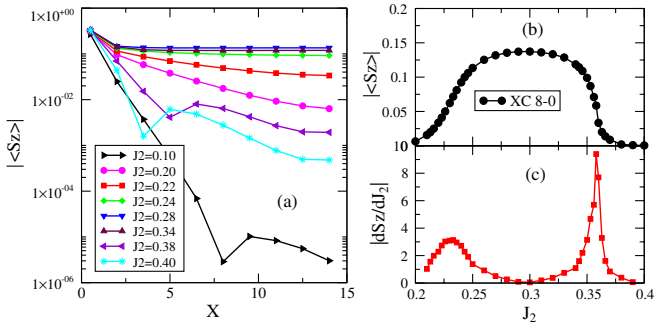

FIG. 3 (color online). (a) Local magnetization $|\langle S_z \rangle|$ versus distance from the end of an XC8 cylinder for various J_2 values. (b) The magnetization at the cylinder center versus J_2. (c) The derivative of the central $|\langle S_z \rangle|$ versus J_2. The peaks of the derivative at $J_2 = 0.23$ and 0.36 indicate the two phase transition points.

an XC8 cylinder with $J_2 = 0.3$. We find that $|\langle S_x \rangle|$ decays exponentially with distance from the cylinder end with a very short correlation length $\xi_x = 1.8$, but $|\langle S_z \rangle|$ rises from the end and saturates in the center of cylinder (not shown). This provides solid evidence that Ising order is very robust on this cylinder. As another test, we have measured the correlation function $|\langle S_i^+(0) S_j^-(x) \rangle|$ and find that its correlation length decreases as a function of increasing J_2 for J_2 near 0.22, and then increases rapidly for J_2 near 0.36. The minimum correlation length is roughly $\xi \sim 1.5$ at $J_2 = 0.3$ (not shown). This result again confirms that xy-plane order is absent in the intermediate phase.

In Fig. 3, we apply a staggered field with $h_z = 0.5$ at a cylinder end to measure the decay of $|\langle S_z \rangle|$ with distance from the end for various values of J_2. As shown in Fig. 3(a), $|\langle S_z \rangle|$ decays exponentially within both the Néel and the dimer phases, but the correlation length gets longer and $|\langle S_z \rangle|$ becomes spatially uniform in the cylinder center for the Ising ordered phase. In Fig. 3(b), we show the magnetization in the cylinder center versus J_2. It is clear from this plot that the intermediate Ising phase is a broad regime, and from its derivative versus J_2, we determine the two phase transition points at ~0.23 and 0.36, which approximately match the phase transitions determined from Fig. 1. It is interesting to note that $|\langle S_z \rangle|$ is almost independent of J_2 for much of this intermediate Ising phase. The moment $|\langle S_z \rangle| \sim 0.14$ is strongly reduced from the maximum "classical" value of 0.5.

The derivative of $|\langle S_z \rangle|$ shown in Fig. 3(c) shows markedly different behavior for the two transitions, with the second transition being much sharper. A natural interpretation is that the phase transition between Néel and Ising phases is continuous, but the second phase transition point is first order. To test this, we have performed calculations on cylinders with a much narrower range of J_2 values along the length of the cylinder, zooming in on the transitions. If the phase transition is first order, we expect that the phase transition region should remain narrow as we zoom in. For a continuous phase transition, the phase transition region should broaden as we zoom in. Varying the gradient of J_2 by a factor of 5, we do find that the Néel-Ising phase transition region broadens, but the second phase transition region stays narrow. Thus, it does appear that the former is continuous, and the latter is first order. However, any conclusions about the second transition are tentative, because of the close competition between the dimer and collinear phases for $J_2 > 0.36$.

To make sure that the Ising order is not a finite size effect, we have studied the $J_2 = 0.3$ system for cylinders with various widths. Figure 4(a) shows $|\langle S_z \rangle|$ as a function of x for XC and YC cylinders. In the inset, we plot the extrapolated magnetization at the cylinder center versus the inverse of the cylinder circumference. For these cylinders, the staggered magnetization is nearly constant with circumference, taking a value of about 0.135–0.142. Thus,

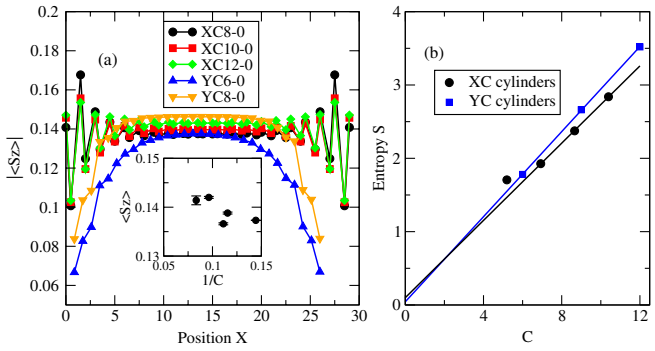

FIG. 4 (color online). (a) The absolute value of the local magnetization $|\langle S_z \rangle|$ for various XC and YC cylinders versus distance along the cylinder. The inset shows the extrapolated magnetization (extrapolated versus the truncation error) at the cylinder center, with error bars, versus the inverse of cylinder circumference C. (b) The entanglement entropy versus circumference for XC and YC cylinders in the intermediate Ising ordered phase at $J_2 = 0.3$. The intercepts are consistent with zero.

we believe that $|\langle S_z \rangle| \sim 0.14$ in the 2D limit for $J_2 = 0.3$. If anything, the staggered magnetization increases with increasing C, so this should be viewed as a lower bound on the value in the 2D limit.

We also measured the entanglement entropy for various cylinder sizes and extrapolated to see if there is a possible topological entanglement entropy contribution (γ) [19,20]; see Fig. 4(b). Entanglement entropy area law states that for a gapped phase $S \sim aL + \gamma + O(1/L)$, with L its boundary length [21]. For a Z_2 spin liquid, one would expect $\gamma = -\ln 2$. We find $\gamma \sim 0.09$ for XC cylinders and $\gamma \sim 0.04$ for YC cylinders, values consistent with zero, as expected for a nontopologically ordered state. We expect that if we could include larger cylinders, the resulting data would extrapolate to $\gamma = 0$.

Very recently, a variational Monte Carlo study of this model has appeared [22]. In Ref. [22], a variational spin-liquid wave function is constructed by decomposing the boson operators into a pair of fermions with a long-range Jastrow factor, with Gutzwiller projection enforcing single occupancy. At $J_2 = 0.3$, the lowest energy for such a state had energy per spin $E = -0.281\,54$, which is ~4% higher than ED of the $4 \times 4 \times 2$ torus ($E = -0.295\,275$) [22]. Although this might appear to be a small difference in energy, for competing phases in geometrically frustrated spin-1/2 models near spin liquids, this is actually a very large energy difference. For example, the spin-1/2 kagome antiferromagnet (with $J_2 = 0$) has an energy difference of only about 1% between the (metastable) honeycomb valence bond crystal and the spin-liquid ground state [7]. In our DMRG calculations, the energy per spin for a specific cylinder geometry can be calculated by subtracting two cylinders with the same width but different lengths [17]. When the cylinder is long enough, this method gives the energy per spin in the cylinder center, with minimal

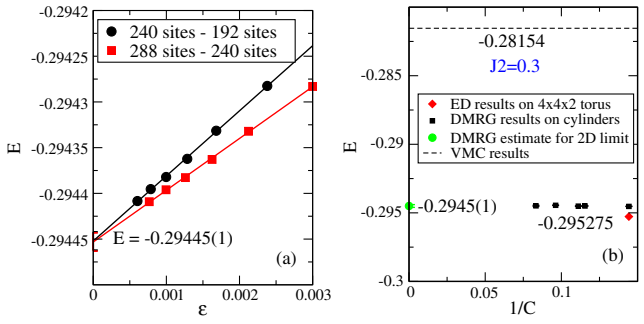

FIG. 5 (color online). (a) The extrapolation of the ground state energy per spin for $J_2 = 0.3$ versus truncation error for the XC12 cylinder. The black curve (circles) is the energy per spin from subtracting the energies of two XC12 cylinders with lengths $L_x = 20$ and $L_x = 16$. The red curve (squares) is from subtracting two cylinders with $L_x = 24$ and $L_x = 20$. These two subtractions extrapolate to the same energy per spin of $-0.294\,45(1)$. (b) The ground state energy per spin for $J_2 = 0.3$ versus the inverse of cylinder circumference from our DMRG calculations, compared with the variational Monte Carlo (VMC) result from Table III in the Supplemental Material of Ref. [22], and exact diagonalization [22].

edge effects. We show in Fig. 5(a) that the energy per spin from subtracting two different pairs of cylinders gives precisely the same energy for the XC12 cylinder. Thus, we find that the ground state energy per spin is $-0.294\,45(1)$ for an infinitely long XC12 cylinder at $J_2 = 0.3$. In Fig. 5(b), we compare our DMRG results for the ground state energy on various cylinders at $J_2 = 0.3$. For the cylinders we study, the DMRG energies have quite small finite size effects. We estimate that the ground state energy is $E = -0.2945(1)$ in the 2D limit. The small-size ED result is only slightly ($\sim 0.26\%$) lower in energy, due to its finite size effects. The state DMRG finds has antiferromagnetic Ising order with the spin moments ordered in the z direction. This ordered ground state has much lower energy than the variational spin-liquid state.

We have not been able to find a simple analytical argument or calculation that gives an intuitive picture for this Ising ordered state. However, viewing the system as hard-core bosons at half filling provides an additional perspective. The Hamiltonian can be mapped straightforwardly and exactly into a hard-core boson model with first-neighbor hopping $t_1 = J_1/4$ and second-neighbor hopping $t_2 = J_2/4$, since $S^\dagger = b^\dagger/2$, $S^z = b^\dagger b - 0.5$. The Ising order would appear as a charge density wave (CDW) order, where the density is higher on sublattice A ($n_A \sim 0.64$) than on sublattice B ($n_B = 1 - n_A \sim 0.36$). Although there are only hopping terms in this hard-core boson Hamiltonian, the hard-core constraint (one boson per lattice site) is an on-site interaction. One could imagine that this on-site interaction renormalizes in some way to produce a first-neighbor density-density interaction, which could produce the CDW. This system is the first that we are aware of where a CDW is produced only from the combination of frustrated hopping and a hard-core constraint.

In summary, we have studied the $J_1 - J_2$ antiferromagnetic spin-1/2 XY model on the honeycomb lattice on various cylinders with DMRG. Instead of a spin-liquid ground state in the intermediate phase regime for $0.22 < J_2/J_1 < 0.36$, we find an Ising ordered phase with a staggered magnetization along the z direction that does not show any strong finite size effects. This Ising order is thus robust on various cylinder circumferences. We obtain a ground state energy much lower than proposed spin-liquid states, and a vanishing topological entanglement entropy. Thinking about this in terms of the spin model, it is somewhat puzzling to understand why this phase appears, since there are no $S_i^z S_j^z$ interaction terms in the spin Hamiltonian. Describing the system instead as hard-core bosons with frustrated hopping, this Ising phase is then a Mott insulator with one boson per two-site unit cell, and the Ising order is then CDW order that breaks the Z_2 sublattice symmetry of the unit cell. The on-site hard-core interaction must induce a first-neighbor repulsion that stabilizes this CDW order. Thus, although this model unfortunately does not appear to exhibit a spin-liquid ground state, it exhibits this somewhat surprising CDW Z_2 ordered phase.

We thank Hongcheng Jiang for early collaboration on this work. We would also like to thank Sasha Chernyshev, Leonid Glazman, Andreas Laeuchli, Sid Parameswaran, Marcos Rigol, Victor Galitski, Leon Balents, Miles Stoudenmire, and Simeng Yan for many helpful discussions. This work was supported by NSF Grant No. DMR-1161348 (Z. Z., S. R. W.), NSF MRSEC Grant No. DMR-0819860 (D. A. H.), and the DARPA OLE program (D. A. H.).

[1] L. Balents, Nature (London) **464**, 199 (2010).
[2] J. S. Helton, K. Matan, M. P. Shores, E. A. Nytko, B. M. Bartlett, Y. Yoshida, Y. Takano, A. Suslov, Y. Qiu, J.-H. Chung, D. G. Nocera, and Y. S. Lee, Phys. Rev. Lett. **98**, 107204 (2007).
[3] M. A. de Vries, K. V. Kamenev, W. A. Kockelmann, J. Sanchez-Benitez, and A. Harrison, Phys. Rev. Lett. **100**, 157205 (2008).
[4] J. S. Helton, K. Matan, M. P. Shores, E. A. Nytko, B. M. Bartlett, Y. Qiu, D. G. Nocera, and Y. S. Lee, Phys. Rev. Lett. **104**, 147201 (2010).
[5] T. H. Han, J. S. Helton, S. Chu, A. Prodi, D. K. Singh, C. Mazzoli, P. Muller, D. G. Nocera, and Y. S. Lee, Phys. Rev. B **83**, 100402(R) (2011).
[6] T. H. Han, J. S. Helton, S. Chu, D. G. Nocera, J. A. R.-Rivera, C. Broholm, and Y. S. Lee, Nature (London) **492**, 406 (2012).
[7] S. Yan, D. A. Huse, and S. R. White, Science **332**, 1173 (2011).
[8] S. Depenbrock, I. P. McCulloch, and U. Schollwock, Phys. Rev. Lett. **109**, 067201 (2012).

[9] H. C. Jiang, Z. H. Wang, and L. Balents, Nat. Phys. **8**, 902 (2012).
[10] C. N. Varney, K. Sun, V. Galitski, and M. Rigol, Phys. Rev. Lett. **107**, 077201 (2011).
[11] D. N. Sheng, O. I. Motrunich, and M. P. A. Fisher, Phys. Rev. B **79**, 205112 (2009).
[12] M. S. Block, D. N. Sheng, O. I. Motrunich, and M. P. A. Fisher, Phys. Rev. Lett. **106**, 157202 (2011).
[13] I. Kimchi, S. A. Parameswaran, A. M. Turner, F. Wang, and A. Vishwanath, Proc. Natl. Acad. Sci. U.S.A. **110**, 16 378 (2013).
[14] T. A. Sedrakyan, L. I. Glazman, and A. Kamenev, arXiv:1303.7272.
[15] S. R. White, Phys. Rev. Lett. **69**, 2863 (1992).
[16] S. R. White, Phys. Rev. B **48**, 10 345 (1993).
[17] E. M. Stoudenmire and S. R. White, Annu. Rev. Condens. Matter Phys. **3**, 111 (2012).
[18] Z. Zhu, D. A. Huse, and S. R. White, Phys. Rev. Lett. **110**, 127205 (2013).
[19] A. Kitaev and J. Preskill, Phys. Rev. Lett. **96**, 110404 (2006).
[20] M. Levin and X. G. Wen, Phys. Rev. Lett. **96**, 110405 (2006).
[21] J. Eisert, M. Cramer, and M. B. Plenio, Rev. Mod. Phys. **82**, 277 (2010).
[22] J. Carrasquilla, A. Di Ciolo, F. Becca, V. Galitski, and M. Rigol, arXiv:1307.2267.